materials

MDPI

Article

Effects of Ion Irradiation and Temperature on Mechanical Properties of GaN Single Crystals under Nanoindentation

Zhaohui Dong [1], Xiuyu Zhang [2], Jingli Li [3], Shengyuan Peng [4], Qiang Wan [5,*], Jianming Xue [4,*] and Xin Yi [3,*]

[1] School of Traffic Management, People's Public Security University of China, Beijing 100038, China; zhdong@ppsuc.edu.cn
[2] Institute of Electronic Engineering, China Academy of Engineering Physics, Mianyang 621999, China; xiuyuzhang@pku.edu.cn
[3] Department of Mechanics and Engineering Science, College of Engineering, Peking University, Beijing 100871, China; lijingli@pku.edu.cn
[4] State Key Laboratory of Nuclear Physics and Technology, School of Physics, Peking University, Beijing 100871, China; 2101110314@pku.edu.cn
[5] Institute of Systems Engineering, China Academy of Engineering Physics, Mianyang 621999, China
* Correspondence: wanzhenyu@126.com (Q.W.); jmxue@pku.edu.cn (J.X.); xyi@pku.edu.cn (X.Y.)

Abstract: Understanding the impact of irradiation and temperature on the mechanical properties of GaN single crystals holds significant relevance for rational designs and applications of GaN-based transistors, lasers, and sensors. This study systematically investigates the influence of C-ion irradiation and temperature on pop-in events, hardness, Young's modulus, and fracture behavior of GaN single crystals through nanoindentation experiments. In comparison with unirradiated GaN samples, the pop-in phenomenon for ion-irradiated GaN samples is associated with a larger critical indentation load, which decreases with increasing temperature. Both unirradiated and ion-irradiated GaN samples exhibit a decline in hardness with increasing indentation depth, while Young's moduli do not exhibit a clear size effect. In addition, intrinsic hardness displays an inverse relationship with temperature, and ion-irradiated GaN single crystals exhibit greater intrinsic hardness than their unirradiated counterparts. Our analysis further underscores the significance of Peierls stress during indentation, with this stress decreasing as temperature rises. Examinations of optical micrographs of indentation-induced fractures demonstrate an irradiation embrittlement effect. This work provides valuable insights into the mechanical behavior of GaN single crystals under varying irradiation and temperature conditions.

Keywords: GaN single crystals; ion irradiation; high-temperature nanoindentation; hardness; mechanical properties

Citation: Dong, Z.; Zhang, X.; Li, J.; Peng, S.; Wan, Q.; Xue, J.; Yi, X. Effects of Ion Irradiation and Temperature on Mechanical Properties of GaN Single Crystals under Nanoindentation. *Materials* **2023**, *16*, 7537. https://doi.org/10.3390/ma16247537

Academic Editor: Fabrizio Roccaforte

Received: 2 November 2023
Revised: 29 November 2023
Accepted: 4 December 2023
Published: 6 December 2023

Copyright: © 2023 by the authors. Licensee MDPI, Basel, Switzerland. This article is an open access article distributed under the terms and conditions of the Creative Commons Attribution (CC BY) license (https://creativecommons.org/licenses/by/4.0/).

1. Introduction

Gallium nitride (GaN), recognized for its wide bandgap, robust interatomic bonds, and exceptional thermal conductivity, stands as a prominent III–V semiconductor material [1]. It finds widespread applications in optoelectronics, high-temperature environments, and high-power devices, including light-emitting diodes, microwave power components, ultra-high-power switches, and laser diodes spanning from blue to the ultraviolet spectrum [2]. GaN crystals, renowned for their resilience to radiation damage [3], are integral to satellite systems, nuclear applications, and various extreme conditions where radiation resistance is paramount. Nevertheless, the microstructural damage incurred by high-energy particle irradiation on GaN crystals inevitably exerts an influence on their mechanical and physical characteristics, eventually impacting device longevity. Furthermore, GaN semiconductor devices frequently encounter elevated temperature during practical deployment. Thus, a comprehensive comprehension of the mechanical implications of radiation damage in

this semiconductor material at high temperature can facilitate the advancement of high-performance and highly reliable GaN-based devices. This holds particular significance as device dimensions shrink to the microscale or below, necessitating a nanoscale understanding of GaN crystal mechanical properties under the combined effects of irradiation and temperature.

Given its low cost, low residual radioactivity, and high damage efficiency [4], ion irradiation experiments offer a suitable avenue for exploring the irradiation effects on GaN semiconductor devices. Nevertheless, the restricted depth of ion irradiation poses challenges when evaluating the macroscopic mechanical properties of irradiated materials using conventional mechanical testing methods like uniaxial tensile and compression tests. Instead, a range of small-scale mechanical testing techniques with high spatial resolution have been employed. Among these, nanoindentation stands out due to its relatively straightforward experimental setup and abundant, insightful data, making it a practical choice for studying the mechanical degradation of materials at the nanoscale [5–7].

At present, there is limited research on the mechanical properties of ion-irradiated GaN materials. While Kavouras et al. [8,9] explored the effects of Si^+, Mg^+, O^+, and N^+ ion implantation on the mechanical properties of epitaxially grown GaN samples using microhardness measurements, their findings were somewhat coarse, as they did not consider the plastic zone under the indenter extending from the ion-irradiated layer to the unirradiated layer. Some researchers have examined the mechanical properties of GaN materials after ion irradiation through experimental nanoindentation. For instance, Kucheyev et al. [10] delved into the pop-in event, hardness, and Young's modulus of wurtzite GaN films modified by 2 MeV $197Au^+$ ion bombardment by nanoindentation with a spherical indenter. Jian et al. [11] studied the hardness and indentation size effects with increasing In concentration in the $In_xGa_{1-x}N$ films. However, they only showed results on the indentation size effect; mechanistic discussions were not provided. Eve et al. [12] investigated the pile-up, hardness, and Young's modulus of GaN films irradiated with swift heavy uranium ions. More recently, our research explored the statistics of pop-in events of GaN single crystals irradiated by 3 MeV C^+ ions, identifying a linear relationship between the regression slop as a micromechanical characterization and the hardness [13]. However, these studies have yet to address the influence of elevated temperature on the mechanical properties of ion-irradiated GaN.

While separate studies have examined the mechanical properties of GaN materials at elevated temperature, the mutual effects of ion irradiation and high temperature on GaN's mechanical properties remain unexplored. Notably, the works by Yonenage et al. [14], Lu et al. [15], and Wheeler et al. [16] have contributed insights into GaN's mechanical behavior under varying conditions, but none have specifically investigated the combined effects of ion irradiation and elevated temperature. In addition, molecular dynamics (MD) simulations have been performed to study the mechanism of plastic deformation in irradiation GaN [17] and temperature effect on the mechanical response of c-plane monocrystalline GaN during nanoindentation [18]. Currently, systematic studies simultaneously probing the effects of ion irradiation and elevated temperature on GaN's mechanical properties are lacking. Such investigations are pivotal for advancing the development of high-performance GaN-based devices.

In this work, systematic nanoindentation measurements from room temperature (RT) to 300 °C have been performed on ion-irradiated and unirradiated GaN single crystals. The influence of ion irradiation and temperature variations on multiple aspects, including the pop-in phenomena, material piling-up, indentation size effect, and fracture behaviors, is explored. The hardness and Young's modulus of all samples are determined. In contrast to face-centered cubic metals like Al and Cu, which exhibit negligible Peierls stress, GaN single crystals exhibit a Peierls stress in the range of a few gigapascals, with a decreasing trend as temperature rises. Additionally, it is shown that irradiation embrittlement effects are significant in GaN single crystals. All samples show no creep behaviors at the tested temperature and irradiation levels. This work advances our understanding of the combined

impacts of irradiation and temperature on the mechanical properties of GaN single crystals, and might aid the rational design of GaN-based transistors, lasers, and sensors.

2. Materials and Methods

2.1. Sample Preparation

Free-standing polar (c-plane) GaN single crystal samples, provided by Suzhou Nanowin Science and Technology Co., Ltd. (Suzhou, China), are prepared by hydride vapor phase epitaxy (HVPE). Each sample has dimensions of 10 mm × 10.5 mm, a thickness of 350 ± 25 μm, and exhibits a surface roughness smaller than 0.2 nm. Values of the sample thickness and surface roughness are provided by the company.

3 MeV C^+ ion irradiation of the GaN single crystal samples is conducted using a 1.7 MV tandem ion accelerator at RT with a fluence of 9.6×10^{15} ions/cm^2. The flux of C^+ ion is controlled at 1×10^{12} ions/(cm^2·s) to minimize significant target heating. The implanted carbon distribution and corresponding displacements-per-atom (dpa) profile are determined using SRIM (stopping and range of ions in matter) simulations [19] with "Quick" Kinchin-Pease option [20] (Figure 1). The dpa versus damage depth profile can be roughly divided into two regions: in region I, the dpa value or damage level gradually increases with depth, while region II displays a rapid variation, signifying a significantly non-uniform damage distribution. To mitigate the influence of this non-uniform damage distribution on the nanoindentation analysis, the indentation depth of the irradiated GaN samples is confined to below 200 nm.

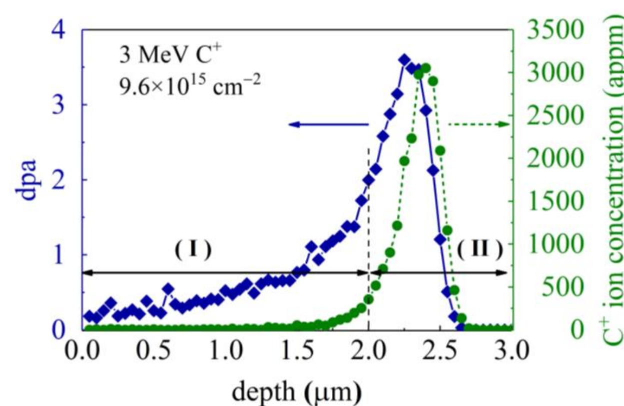

Figure 1. C^+ ion concentration and dpa profiles determined using SRIM calculations for GaN implanted with C^+ at 3 MeV with an ion fluence of 9.6×10^{15}/cm^2. The irradiation-induced damage extends to a depth of approximately 3 μm, with the peak damage occurring at a depth of about 2.25 μm beneath the sample surface. appm, atomic parts per million.

2.2. Nanoindentation Procedure and Analysis

High-temperature nanoindentation tests on both unirradiated and ion-irradiated samples are performed using a Hysitron TI 980 Triboindenter (Bruker, Minneapolis, MN, USA) equipped with an xSol 800 heating stage [21] and integrated with a scanning probe microscopy (SPM) system. As tip-shape controls performed after tests at temperature from RT to 300 °C show no change in area function [22], in this study, the area function and machine compliance are calibrated at RT on fused quartz, following the ISO14577 standard procedure [23]. The Berkovich indenter is affixed to a low-thermal-conductivity shaft to reduce heat transfer from the surface to the transducer and prevent the oxidation or melting of the standard probe holder at high temperature [24]. The sample is sandwiched and heated using resistance heating plates. Each heating plate is equipped with a thermocouple to measure and control the testing temperature and is also equipped with a water coolant and environmental gas flow system. The heating rate is controlled by the equipment software, with an average heating rate of 20 °C/min. The sample is first heated to a selected target temperature and a holding time of around ten minutes is required to reach

thermal equilibrium due to the excellent thermal stability of the xSol heating stage. In the high-temperature nanoindentation experiments, high-purity nitrogen gas (>99.9992%) is used to shield the GaN sample surface from oxidation. To maintain thermal equilibrium and minimize thermal drift, the probe is positioned 10 μm above the sample surface before each indentation test.

Nanoindentation tests of unirradiated and ion-irradiated samples are carried out at RT, 100 °C, 200 °C, and 300 °C with a load-controlled partial unloading/cyclical mode. The load function contains a total of ten partial unloading cycles, and each cycle comprises three consecutive segments of 0.4 s loading, 0.1 s holding, and 0.5 s unloading. The minimum loading force, maximum loading force, cyclic loading exponent, and unloading fraction are 3 mN, 12 mN, 1, and 0.5, respectively. At least ten indents are performed on individual samples at each temperature, and average values of the hardness H and reduced Young's modulus E^* are calculated. The space separation between indents is large enough to avoid plastic zone interaction. Once load–displacement curves are obtained, the hardness H and reduced Young's modulus E^* at different values of temperature and indentation depth are determined from the unloading part using the Oliver and Pharr method as [25]

$$H = \frac{P}{A}, \tag{1}$$

$$E^* = \frac{\sqrt{\pi}}{2\beta} \frac{S}{\sqrt{A}}, \tag{2}$$

where P is the indenter load, A is the projected area of contact whose value depends on the indenter geometry and contact depth, the indenter geometry shape factor β is taken as 1.034 for Berkovich indenter [11,26], and $S = \mathrm{d}P/dh|_{h=h_{\max}}$ is the contact stiffness. The indenter area function $A(h_c)$ takes the form [25]

$$A = C_0 h_c^2 + C_1 h_c + C_2 h_c^{1/2} + C_3 h_c^{1/4} + C_4 h_c^{1/8} + \ldots, \tag{3}$$

where h_c is the depth of circle of contact measured from maximum depth $h_{\max}$ (contact depth). Before the nanoindentation measurements, indentations are first performed on a fused silica sample to determine values of coefficients C_0 (=24.5 for an ideal Berkovich tip), C_1, C_2, $\cdots$, etc. The constants C_k (k = 1, 2, $\cdots$) are coefficients determined by fitting measured A versus h_c data, and their associated terms in Equation (3) depict deviations from the ideal Berkovich geometry due to blunting at the tip. Once E^* is determined, the Young's modulus E_{GaN} of GaN samples could be obtained from

$$\frac{1}{E^*} = \frac{1-\nu_i^2}{E_i} + \frac{1-\nu_{GaN}^2}{E_{GaN}}, \tag{4}$$

where ν_i and E_i denote the Poisson ratio and Young's modulus of the indenter tip, respectively, and ν_{GaN} is the Poisson ratio of the GaN samples, which is taken as 0.25 [27]. For diamond indenters used here, E_i = 1141 GPa and ν_i = 0.07.

The Berkovich diamond probe is also used as an SPM tip to in situ measure the sample surface topography. The SPM made it possible to examine and measure the pile-ups. The presence of pile-ups at the periphery of the contact impression would affect the evaluation of contact area and the subsequent hardness. By approximating the pile-up contact perimeter as a semi-ellipse, the true contact area A_s of the indentation for irradiated GaN single crystals with evident pile-ups is given by [28]

$$A_s = A + 5.915 h_c \sum a_j \ (j = 1, 2, 3), \tag{5}$$

where A and h_c are obtained using the Oliver–Pharr method [25], and a_j is the horizontal distance between the pile-up contact perimeter to the edge of the indentation, with j = 1, 2, and 3 denoting the three semi-elliptical projected pile-up lobes. Replacing the contact

area A in Equation (3), the true contact area A_s given by Equation (5) is used to calculate the hardness of the irradiated GaN single crystals.

To study the effects of irradiation and temperature on the fracture behaviors of GaN single crystals, the load-controlled indents are applied with larger loads, involving a trapezoidal loading sequence: 5 s linear loading, 2 s holding segment at the peak load, and 5 s linear unloading. The maximum load is set as 3 N, and each temperature condition is tested with a minimum of three indents on individual samples. The crack morphology is examined promptly after the nanoindentation tests.

Nanoscale Dynamic Mechanical Analysis (nanoDMA) is a technique used to analyze the dynamic mechanical properties of materials at the nanoscale, encompassing attributes like energy dissipation and time-dependent deformation characteristics. To study the influence of irradiation and temperature on the creep behaviors of GaN single crystals, nanoDMA tests are carried out. These tests employ specific parameters: a peak force of 12 mN, a frequency of 220 Hz, a load amplitude of 120 µN, and a total test time of 600 s. At least three indents are performed on individual samples at each temperature. Once the indentation experiments at a selected temperature are finished, the temperature is increased to the next selected value. The time interval between tests at different temperatures is within one hour.

3. Results

3.1. Effects of Temperature and Ion Irradiation on Pop-In Load

Figure 2 shows the typical partial unloading/cyclical load–penetration depth (P–h) curves performed at RT, 100 °C, 200 °C, and 300 °C. The range of the indentation force is from 3 mN to 12 mN. Under a maximum loading force of 12 mN, the unirradiated GaN single crystals exhibit a notable increase in indentation depth, with h progressing from 172.22 nm at RT to 200 nm at 300 °C, signifying a 16.1% increment. In contrast, the ion-irradiated GaN single crystals demonstrate a more modest rise in h, registering a 7.5% increase, from 158.88 nm at RT to 170.82 nm at 300 °C, under P = 12 mN. Since the maximum indentation depth h_{max} is around 200 nm, significantly smaller than the thickness of the damage region I as depicted in Figure 1, the substrate effect could be neglected.

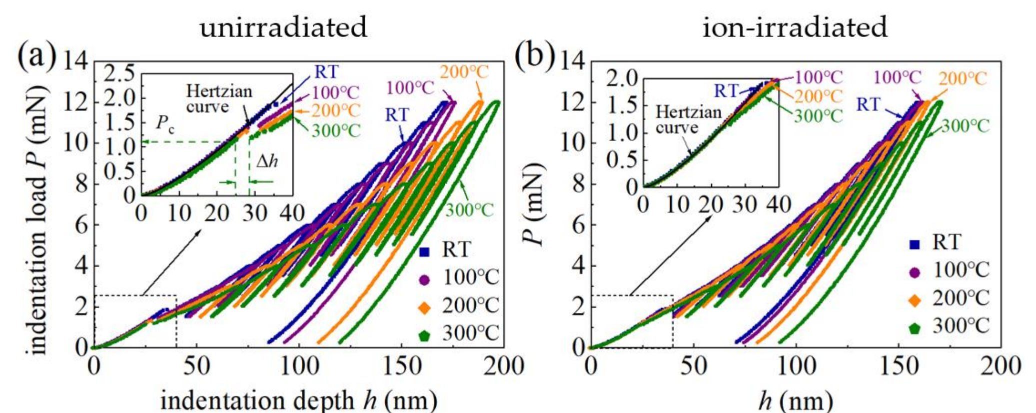

Figure 2. Partial unloading/cyclical curves of (**a**) the unirradiated and (**b**) ion-irradiated GaN single crystal samples for indents performed at RT, 100 °C, 200 °C, and 300 °C, with a force range from 3 mN to 12 mN. Insets, magnified view of first pop-in discontinuities.

The pop-in phenomena (sudden displacement jump) in P–h curves are observed at shallow indentation depths (Figure 2). Similar pop-in phenomena have been observed in nanoindentation of GaN single crystals [13,29,30], GaN thin films on substrates [31], and as well as many other brittle semiconductor materials (e.g., Si, InP, ZnO, and GaAs) [32]. The first pop-in events in GaN single crystals under nanoindentation are associated with the critical transition from pure elastic behavior to plastic deformation [14] and are usually attributed to dislocation nucleation and propagation during loading [32]. This is reflected

in *P*–*h* curves in Figure 2, which are well characterized by the agreement with and deviation from the Hertzian relationship before and after the first pop-in phenomenon. The load at the occurrence of the first pop-in event is recorded as the critical load P_c, and the sudden displacement jump Δh is recorded as the displacement excursion (Figure 2a). The average critical loads P_c of the unirradiated and ion-irradiated samples as functions of temperature are shown in Figure 3, and the error bars represent the standard deviations of at least ten measurements per temperature. These values are included in Table 1.

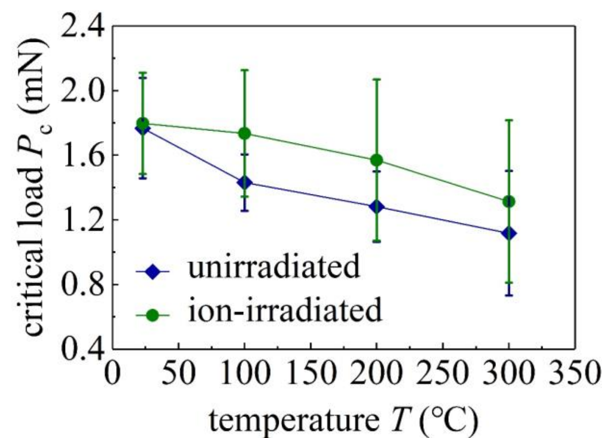

Figure 3. Critical loads P_c of unirradiated and ion-irradiated GaN single crystals at different temperature *T*. Error bars, standard deviations.

Table 1. Measured mechanical properties of unirradiated and irradiated GaN single crystals by nanoindentation at different temperature *T*.

T (°C)	Unirradiated				Ion-Irradiated			
	P_c (mN)	E_{GaN} (GPa)	H_0 (GPa)	*h** (nm)	P_c (mN)	E_{GaN} (GPa)	H_0 (GPa)	*h** (nm)
RT	1.77 ± 0.31	269.5 ± 3.1	15.81	33.89	1.80 ± 0.31	261.9 ± 1.7	21.16	17.58
100	1.43 ± 0.17	270.2 ± 3.1	14.60	39.70	1.73 ± 0.39	262.1 ± 2.9	19.42	20.87
200	1.28 ± 0.22	264.6 ± 3.9	12.52	51.18	1.57 ± 0.50	259.5 ± 3.2	18.47	22.65
300	1.12 ± 0.39	252.7 ± 3.7	10.68	63.90	1.42 ± 0.50	250.6 ± 2.2	17.19	24.62

The first pop-in events in GaN single crystals are primarily associated with the sudden nucleation and propagation of dislocations gliding along the most active slip systems [31,33]. Defects in the disordered layer of the ion-irradiated GaN single crystals may act as dislocation pinning points [10]. The extent to which the dislocations are pinned may affect the critical load P_c. Figure 3 shows that, at the same temperature, the average value of P_c of the ion-irradiated samples is larger than that of the unirradiated samples, and values of P_c of both the unirradiated and ion-irradiated samples decrease as the temperature *T* increases. These results are consistent with the nanoindentation of ion-bombarded modified wurtzite GaN films [10], showing that the elastic behaviors of ion-irradiated GaN samples extend to higher loads than unirradiated GaN samples. As the nucleation and propagation of dislocations are stress-assisted and thermally activated, the statistical distribution of the pop-in phenomenon is affected by both temperature and loading rate. Since the loading rate remains constant in this study, the reduction in the average critical load P_c for the unirradiated or ion-irradiated samples is mainly caused by the increasing temperature.

3.2. Effects of Temperature and Ion Irradiation on Young's Modulus

Figure 4 shows Young's moduli E_{GaN} of both unirradiated and ion-irradiated GaN single crystals, exhibiting no clear indentation size effects, which further ensures the

accuracy of the measured hardness shown below. The average values of E_{GaN} of the unirradiated and ion-irradiated GaN samples at different values of T are shown in Figure 5 and are also listed in Table 1. As the temperature T increases from RT to 100 °C, E_{GaN} remains at the same value. In contrast, E_{GaN} slightly decreases as T increases from 100 °C to 300 °C. At RT, the E_{GaN} of the unirradiated GaN samples is 269.5 ± 3.1 GPa (Table 1), in good agreement with reported experimental values [12,27,29], and a there is a reduction of 2.8% upon the C ion irradiation. The ion irradiation-induced slight reduction in Young's modulus has also been observed in the nanoindentation of SiC samples with a Young's modulus reduction of less than 5% after ion irradiation [4]. Such a slight reduction in Young's modulus is attributed to an increase in the atomic spacing caused by irradiation [4].

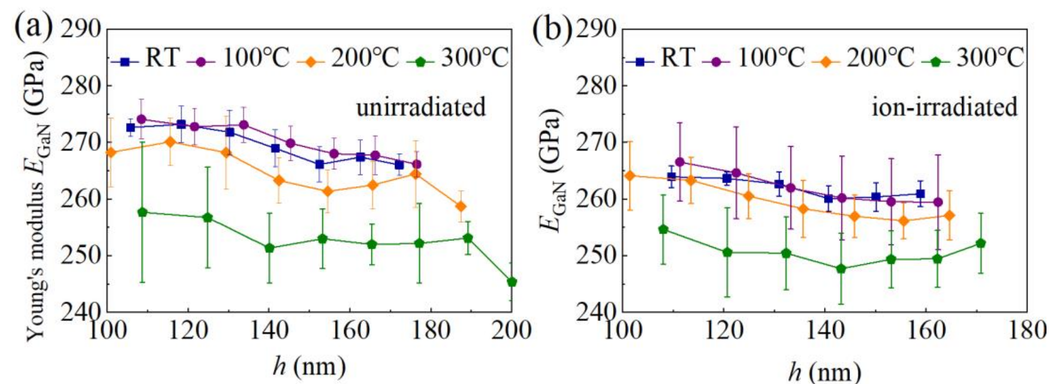

Figure 4. Young's moduli E_{GaN} of unirradiated (**a**) and ion-irradiated (**b**) GaN single crystal samples versus the indentation depth at different temperatures. Error bars, standard deviations.

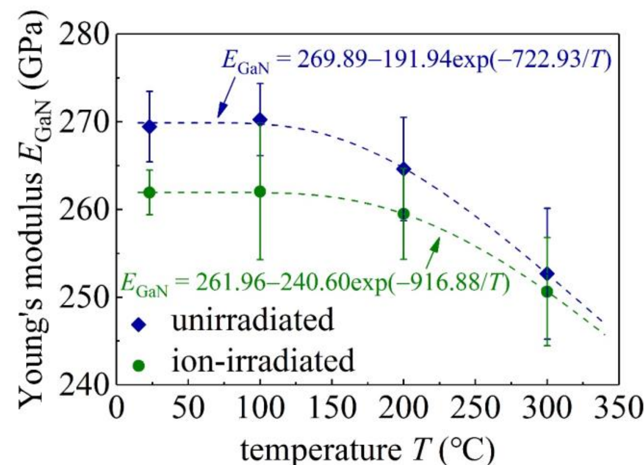

Figure 5. Average Young's moduli E_{GaN} in Figure 4 at different values of T. Error bars, standard deviations.

3.3. Effects of Temperature and Ion Irradiation on Hardness

Evident pile-ups of material around the indentation could be observed for the ion-irradiated GaN single crystals in comparison with the unirradiated GaN samples (Figure 6), consistent with reported nanoindentation results of GaN thin films upon irradiation with swift heavy uranium ions [12]. In addition, all samples show no creep behavior at the tested temperatures.

Figure 7 shows the hardness H of GaN samples as a function of the indentation depth h. As h increases, H decreases, a typical feature of the indentation size effect. As shown in Figure 7, the hardness H of the unirradiated GaN single crystals at RT for indentation depth h = 172 nm is 20.1 GPa, which is consistent with the hardness value 20 ± 1 GPa of unirradiated GaN thin films measured by nanoindentation at an indentation depth of 200 nm reported in the literature [12], and is also consistent with the hardness value

19.2 ± 0.2 GPa of unirradiated GaN single crystals measured by nanoindentation $h = 160$ nm in our recent studies [13]. The hardness of GaN samples measured in the literature may be different due to the different quality of the GaN samples. Considering the generation of geometrically necessary dislocations (GNDs) underneath the indenter, the classical Nix–Gao model predicts the depth-dependent hardness H as [34]

$$H/H_0 = (1 + h^*/h)^{1/2}, \tag{6}$$

where H_0 is the hardness without the presence of GNDs and $h^* = 40.5b\alpha^2\tan^2\theta(\mu/H_0)^2$ is a length characterizing the depth dependence of hardness, depending on the magnitude b of the Burgers vector and shear modulus μ of the material, coefficient α, the angle θ between the surface of the specimen plane and Berkovich indenter, and H_0. In the Nix–Gao model, the effect of intrinsic lattice resistance or Peierls stress on the hardness is ignored. As the Peierls stress is very small for Al and Cu, the Nix–Gao model is well justified for these face-centered cubic metals [35–37].

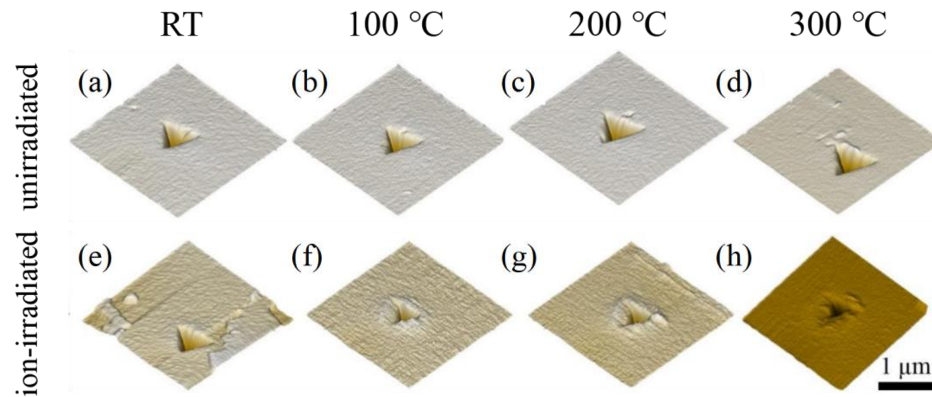

Figure 6. Images of surface topography of the indentation sites for unirradiated (**a**–**d**) and ion-irradiated (**e**–**h**) GaN single crystals at RT (**a**,**e**), 100 °C (**b**,**f**), 200 °C (**c**,**g**), and 300 °C (**d**,**h**).

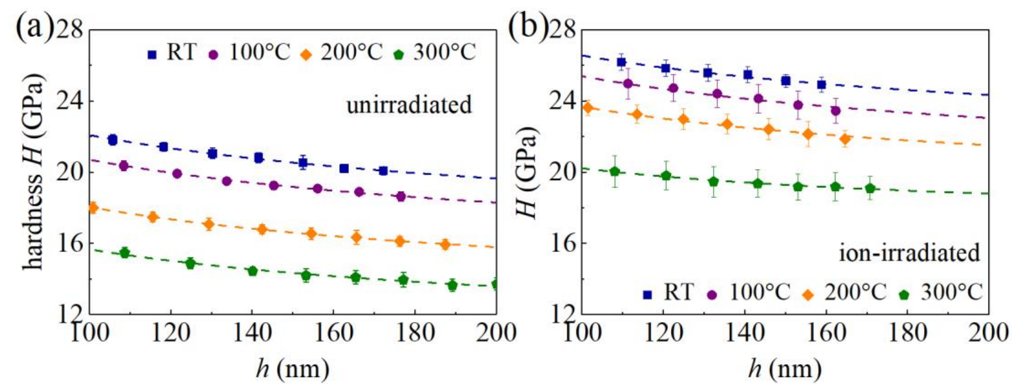

Figure 7. Profiles of the hardness H versus indentation depth h for unirradiated (**a**) and ion-irradiated (**b**) GaN single crystals at different temperatures. Symbols, experimental values; dashed curves, fitting results from Equation (7); error bars, standard deviations.

For GaN single crystals, the Peierls stresses of dislocations of different slip systems are of at least 0.3373 GPa, and the maximum value could reach 27.8631 GPa [38]. Therefore, the Peierls stresses of GaN cannot be ignored. Based on the Nix–Gao model, while taking into account the Peierls stress τ_0, the hardness H as a function of the indentation depth h is given as [39]

$$H = MC\tau_0 + MC\alpha\mu b\sqrt{\rho_{\text{SSD}} + \rho_{\text{GND}}(h)}, \tag{7}$$

where the Taylor factor M is taken as $\sqrt{3}$, the Tabor factor C is taken as 3, α = 0.5, the shear modulus $\mu = E_{GaN}/[2(1 + \nu_{GaN})]$ with ν_{GaN} = 0.25 [27], b = 3.191 Å [40], ρ_{SSD} is the density of statistically stored dislocations (SSDs), and the GND density is $\rho_{GND}(h) = 3\tan^2\theta/(2bh)$ with θ = 24.73°. Fitting experimental data in Figure 7 with Equation (7), values of τ_0 and ρ_{SSD} at different values of T are determined and are shown in Figure 8. For unirradiated GaN samples at RT, τ_0 = 2.35 GPa, falling in a range from 0.34 GPa to 27.86 GPa based on MD simulations [40]. As T increases, τ_0 of the unirradiated GaN samples decreases to 1.13 GPa at 300 °C, and τ_0 of the ion-irradiated GaN samples decreases from 3.19 GPa at RT to 1.28 GPa at 300 °C. The Peierls stress τ_0 becomes larger after irradiation due to the pinning effect induced by the irradiation-induced defects.

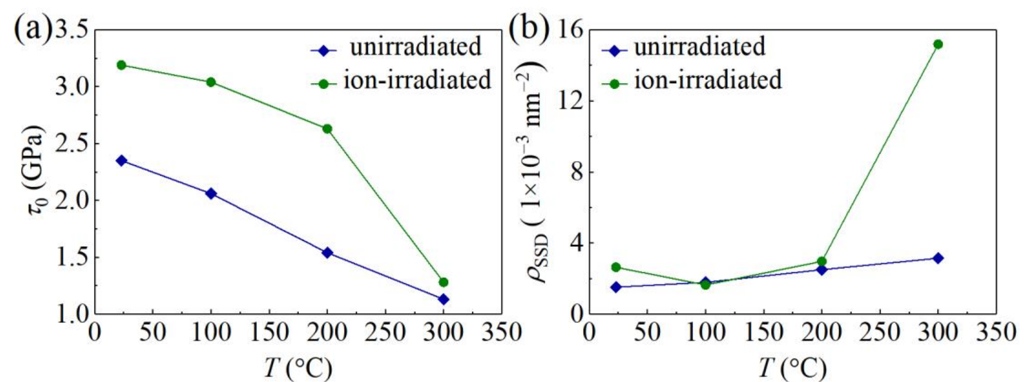

Figure 8. (**a**) τ_0 and (**b**) ρ_{SSD} of unirradiated and ion-irradiated GaN samples at different values of temperature T.

The classical indentation hardness or intrinsic hardness H_0 without the presence of GNDs is

$$H_0 = MC\tau_0 + MC\alpha\mu b\sqrt{\rho_{SSD}}. \quad (8)$$

Values of H_0 of the unirradiated and ion-irradiated GaN samples at different values of T are listed in Table 1 and the corresponding H_0–T curves are plotted in Figure 9a. It is shown that the H_0 of the ion-irradiated GaN single crystals is larger than that of unirradiated GaN sample at the same temperature, indicating an ion irradiation hardening effect. This phenomenon has been consistently observed in GaN subjected to ion irradiation with O^+, N^+, Mg^+, and Si^+ ions [8,9]. The increased hardness is attributed to irradiation-induced defects that effectively immobilize dislocations and impede plastic deformation. Nanoindentation tests on ion-irradiated GaN single crystals reveal the concurrent presence of both the indentation size effect and irradiation hardening.

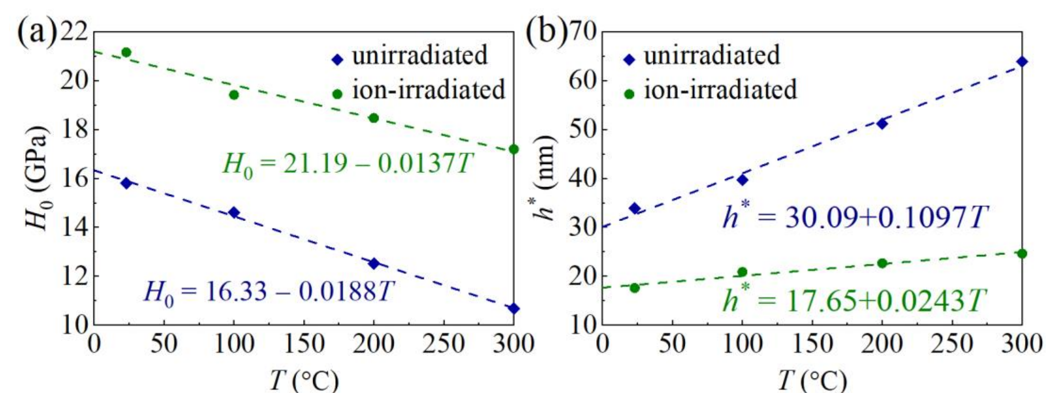

Figure 9. Effects of temperature and irradiation on H_0 (**a**) and h^* (**b**). Dashed lines, linear fitting.

The intrinsic hardness H_0 linearly decreases with increasing T (Figure 9a). For the unirradiated GaN single crystals, H_0 = 16.33 − 0.0188T, a reduction of 32.4% from RT to 300 °C;

for the ion-irradiated GaN single crystals, H_0 = 21.19 − 0.0137T, a reduction of 18.7% from RT to 300 °C. The linear decrease in intrinsic hardness H_0 of the unirradiated GaN single crystals with increasing temperature T aligns with reported MD simulation results [18]. Due to the relatively high Peierls stress τ_0 in GaN, the dislocations move slowly, and the dislocation cross-slip enhances the likelihood of forming dislocation networks [38,41]. As T rises, increased thermal energy facilitates thermal activation over the Peierls barrier, leading to reduced lattice friction or Peierls stress for dislocation motion. According to Equation (8), the decreasing hardness of GaN with increasing T might be linked to the diminishing Peierls stress τ_0 [15,39]. Comparable linear decreases in intrinsic hardness from RT to 400 °C have been observed in various materials, including tungsten, tungsten carbide, diamond, and boron nitride [42,43]. However, over a broader temperature range from RT to 1000 °C, a nonlinear hardness–temperature relationship becomes apparent [42]. Further mechanistic studies are necessary to unveil the intricacies of the hardness–temperature relationship.

A combination of Equations (7) and (8) leads to [39]

$$\frac{H}{H_0} = \frac{MC\tau_0}{H_0} + \sqrt{\left(1 - \frac{MC\tau_0}{H_0}\right)^2 + \frac{h^*}{h}}, \tag{9}$$

where h^* in Equation (9) has the same expression as that in the Nix–Gao model, but it also depends on the Peierls stress via H_0. Fitting the experimental data in Figure 9 with Equation (9), values of h^* at different T can be obtained (Figure 9b and Table 1). Then, the $(H/H_0)^2 - 1/h$ relationship can be obtained (Figure 10).

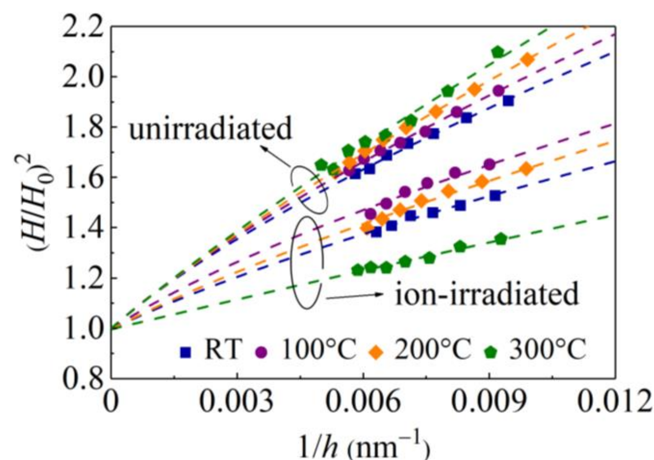

Figure 10. Normalized hardness $(H/H_0)^2$ versus the inverse indentation depth $1/h$ for unirradiated and ion-irradiated GaN single crystals at different temperatures. Symbols, experimental values; dashed curves represent fitting results from Equation (9).

3.4. Effects of Temperature and Ion Irradiation on Fracture

Figure 11 shows optical micrographs of residual impression with indentation-induced cracking in unirradiated and ion-irradiated GaN single crystals at a maximum load of 3 N for all tested temperatures. At RT, radial cracks emanate from three corners of the Berkovich indentation print, and the radial cracks in the ion-irradiated GaN single crystals are significantly shorter than these in the unirradiated GaN single crystals (Figure 11a,e). Notably, the residual impression of ion-irradiated GaN single crystals at RT is smaller than that of the unirradiated samples. Three-dimensional MD simulation results of c-plane monocrystalline GaN under nanoindentation show that the nucleation and propagation of dislocations in the main slip systems are promoted to intensify the plastic deformation of the GaN crystal [18]. As shown in the results of the high-temperature nanoindentation tests (Figure 11b–d), the residual impression in the unirradiated GaN single crystals becomes

larger as temperature increases. In the unirradiated GaN single crystals, the radial cracks emanating from three corners of the Berkovich indentation print at 100 °C (Figure 11b) become larger than those at RT (Figure 11a). However, the brightening areas in unirradiated GaN single crystals (Figure 11a) caused by specular reflection at the lateral subsurface cracks disappear at high temperature (Figure 11b–d). The length of the radial cracks of unirradiated GaN single crystals at 200 °C (Figure 11c) changes little compared with that at 100 °C. However, a radial crack from one corner of the Berkovich indentation print of unirradiated GaN single crystals at 200 °C (Figure 11c) disappears. Further, all the radial cracks of unirradiated GaN single crystals at 300 °C disappear. As the temperature increases, the brittleness of unirradiated GaN single crystals tend to weaken. For ion-irradiated GaN single crystals at high temperature (Figure 11f–h), as the temperature increases, the residual impression becomes slightly larger, the radial cracks from the corners seem to be independent of temperature, and erratically shaped small radial cracks begin to appear both from the corners and edges of the Berkovich indentation print.

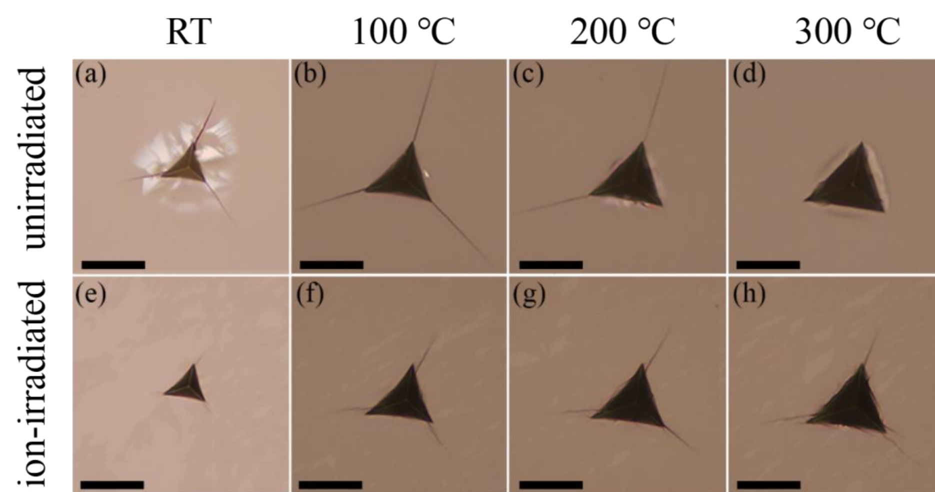

Figure 11. Optical micrographs of residual contact impression with indentation-induced cracking in unirradiated (**a**–**d**) and ion-irradiated (**e**–**h**) GaN single crystals at a maximum load of 3 N for RT (**a**,**e**), 100 °C (**b**,**f**), 200 °C (**c**,**g**), and 300 °C (**d**,**h**). Scale bars, 20 µm.

It has been demonstrated that irradiation-induced residual stress can inhibit crack formation during nanoindentation [44]. However, with an increase in temperature, these residual stresses tend to gradually dissipate. Consequently, a noticeable trend emerges, where the brittleness of ion-irradiated and unirradiated GaN single crystals exhibits opposite behaviors as temperature rises. Specifically, at RT, radial and lateral cracks in ion-irradiated GaN single crystals are notably smaller in comparison to unirradiated samples (Figure 11a,e). In contrast, at 300 °C, unirradiated GaN single crystals exhibit no radial or lateral cracks, whereas radial cracks originating from the corners and edges of ion-irradiated GaN samples remain apparent (Figure 11d,h). This observation, while excluding the influence of residual stress, suggests that irradiation elevates the ductile-to-brittle transition temperature of GaN single crystals, indicating the presence of irradiation-induced embrittlement effects. Furthermore, as temperature increases, it becomes evident that the residual impressions on both unirradiated and ion-irradiated GaN single crystals gradually enlarge, indicating enhanced plasticity at higher temperatures.

4. Conclusions

Systematic experimental investigations on the effects of C ion irradiation and temperature on the hardness, Young's modulus, and fracture of GaN single crystals under nanoindentation have been performed. It is found that the critical indentation load for the occurrence of the pop-in phenomenon decreases as the temperature increases. Moreover, ion-irradiated GaN samples have a larger critical load for pop-in in comparison with unirra-

diated samples, suggesting that the dislocation nucleation or propagation is suppressed by the irradiation-induced defects. For the hardness of both unirradiated and ion-irradiated GaN samples, the typical feature of the indentation size effect is observed, that is, the hardness decreases with the increasing indentation depth. In contrast, Young's moduli of both unirradiated and ion-irradiated GaN single crystals do not exhibit a clear size effect. In addition, the macroscopic hardness decreases as the temperature increases, attributed to the decreasing Peierls stress with increasing temperature. As irradiation-induced defects could pin dislocations and prohibit the plastic deformation, the ion-irradiated GaN single crystals have a larger macroscopic hardness than that of unirradiated samples. Optical micrographs of indentation-induced fracture further indicate irradiation embrittlement effects. No creep behaviors are observed at tested temperatures. Our studies aid understanding the mechanical effects of irradiation damage on GaN single crystals and might have broad implications in improving the service life of GaN-based devices.

Author Contributions: Conceptualization, Z.D. and X.Y.; methodology, Z.D., X.Z., J.L., S.P., J.X., Q.W. and X.Y.; investigation, Z.D., X.Z., J.L., S.P., Q.W., J.X. and X.Y.; writing—original draft preparation, Z.D.; writing—review and editing, X.Y.; supervision, X.Y.; funding acquisition, X.Y. All authors have read and agreed to the published version of the manuscript.

Funding: This research was funded by the National Natural Science Foundation of China (Grant Nos. 11988102 and U1830121) and the Fundamental Research Funds for the Central Universities, China (Grant No. 2022JKF433).

Institutional Review Board Statement: Not applicable.

Informed Consent Statement: Not applicable.

Data Availability Statement: Data are contained within the article.

Conflicts of Interest: The authors declare no conflict of interest.

References

1. Mukai, T.; Nakamura, S. Ultraviolet InGaN and GaN single-quantum-well-structure light-emitting diodes grown on epitaxially laterally overgrown GaN substrates. *Jpn. J. Appl. Phys.* **1999**, *38*, 5735. [CrossRef]
2. Pearton, S.J.; Zolper, J.C.; Shul, R.J.; Ren, F. GaN: Processing; defects; devices. *J. Appl. Phys.* **1999**, *86*, 1–78. [CrossRef]
3. Polyakov, A.Y.; Pearton, S.J.; Frenzer, P.; Ren, F.; Liu, L.; Kim, J. Radiation effects in GaN materials and devices. *J. Mater. Chem. C* **2013**, *1*, 877. [CrossRef]
4. Chen, X.; Zhou, W.; Zhang, X.; Feng, Q.; Zheng, J.; Liu, X.; Tang, B.; Li, J.; Xue, J.; Peng, S. Mechanical properties of 6H-SiC irradiated by neutron and MeV heavy ions: A nanoindentation and finite element method study. *J. Appl. Phys.* **2018**, *123*, 025104. [CrossRef]
5. Gouldstone, A.; Chollacoop, N.; Dao, M.; Li, J.; Minor, A.M.; Shen, Y.L. Indentation across size scales and disciplines: Recent developments in experimentation and modeling. *Acta Mater.* **2007**, *55*, 4015. [CrossRef]
6. Xiao, X.; Yu, L. Nano-indentation of ion-irradiated nuclear structural materials: A review. *Nucl. Mater. Energy* **2020**, *22*, 100721. [CrossRef]
7. Gorji, N.E.; O'Connor, R.; Brabazon, D. X-ray tomography, AFM and nanoindentation measurements for recyclability analysis of 316L powders in 3D printing process. *Procedia Manuf.* **2020**, *47*, 1113. [CrossRef]
8. Kavouras, P.; Katsikini, M.; Vouroutzis, N.; Lioutas, C.B.; Paloura, E.C.; Antonopoulos, J.; Karakostas, T. Ion implantation effects on the microhardness and microstructure of GaN. *J. Cryst. Growth* **2001**, *230*, 454. [CrossRef]
9. Kavouras, P.; Katsikini, M.; Kehagias, T.; Paloura, E.C.; Komninou, P.; Antonopoulos, J.; Karakostas, T. A parametric study of implantation-induced variations on the mechanical properties of epitaxial GaN. *J. Phys. Condens. Matter.* **2002**, *14*, 12953. [CrossRef]
10. Kucheyev, S.O.; Bradby, J.E.; Williams, J.S.; Jagadish, C.; Swain, M.V.; Li, G. Deformation behavior of ion-beam-modified GaN. *Appl. Phys. Lett.* **2001**, *78*, 156. [CrossRef]
11. Jian, S.-R.; Fang, T.-H.; Chuu, D.-S. Nanomechanical characterizations of InGaN thin films. *Appl. Surf. Sci.* **2006**, *252*, 3033. [CrossRef]
12. Eve, S.; Moisy, F.; Germanicus, R.C.; Grygiel, C.; Hug, E.; Monnet, I. Caractérisation par nanoindentation du GaN irradié par des ions uranium de grandeénergie. *Matér. Tech.* **2017**, *105*, 108. [CrossRef]
13. Dong, Z.; Zhang, X.; Peng, S.; Jin, F.; Wan, Q.; Ming, J.; Yi, X. Mechanical properties of GaN single crystals upon C ion irradiation: Nanoindentation analysis. *Materials* **2022**, *15*, 1210. [CrossRef]

14. Yonenage, I.; Hoshi, T.; Usui, A. High temperature hardness of bulk single crystal GaN. *MRS Internet J. Nitride Semicond. Res.* **2000**, *5*, 343. [CrossRef]
15. Lu, J.; Ren, H.; Deng, D.; Wang, Y.; Chen, K.J.; Lau, K.; Zhang, T. Thermally activated pop-in and indentation size effects in GaN films. *J. Phys. D* **2012**, *45*, 085301. [CrossRef]
16. Wheeler, J.M.; Niederberger, C.; Tessarek, C.; Christiansen, S.; Michler, J. Extraction of plasticity parameters of GaN with high temperature, in situ micro-compression. *Int. J. Plast.* **2013**, *40*, 140. [CrossRef]
17. Qian, Y.; Shang, F.; Wan, Q.; Yan, Y. The mechanism of plastic deformation in intact and irradiated GaN during indentation: A molecular dynamics study. *Comput. Mater. Sci.* **2018**, *149*, 230. [CrossRef]
18. Guo, J.; Chen, J.; Wang, Y. Temperature effect on mechanical response of c-plane monocrystalline gallium nitride in nanoindentation: A molecular dynamics study. *Ceram. Int.* **2020**, *46*, 12686. [CrossRef]
19. Ziegler, J.F.; Ziegler, M.D.; Biersack, J.P. SRIM-the stopping and range of ions in matter. *Nucl. Instrum. Methods Phys. Res. B* **2010**, *268*, 1818. [CrossRef]
20. Stoller, R.E.; Toloczko, M.B.; Was, G.S.; Certain, A.G.; Dwaraknath, S.; Garner, F.A. On the use of SRIM for computing radiation damage exposure. *Nucl. Instrum. Methods Phys. Res. B* **2013**, *310*, 75. [CrossRef]
21. Hangen, B.U.; Chen, C.; Richter, A. Mechanical characterization of PM2000 oxide-dispersion-strengthened alloy by high temperature nanoindentation. *Adv. Eng. Mater.* **2015**, *17*, 1683. [CrossRef]
22. Broitman, E.; Tengdelius, L.; Hangen, U.D.; Lu, J.; Hultman, L.; Högberg, H. High-temperature nanoindentation of epitaxial ZrB2 thin films. *Scr. Mater.* **2016**, *124*, 117. [CrossRef]
23. *ISO 14577—1:2015*; Metallic Materials—Instrumented Indentation Test for Hardness and Materials Parameters—Part 1: Test method. ISO: Geneva, Switzerland, 2015.
24. Li, Y.; Fang, X.; Xia, B.; Feng, X. In situ measurement of oxidation evolution at elevated temperature by nanoindentation. *Scr. Mater.* **2015**, *103*, 61. [CrossRef]
25. Oliver, W.C.; Pharr, G.M. An improved technique for determining hardness and elastic modulus using load and displacement sensing indentation experiments. *J. Mater. Res.* **1992**, *7*, 1564. [CrossRef]
26. King, R.B. Elastic analysis of some punch problems for a layered medium. *Int. J. Solids Struct.* **1987**, *23*, 1657. [CrossRef]
27. Nowak, R.; Pessa, M.; Suganuma, M.; Leszczynski, M.; Grzegory, I.; Porowski, S.; Yoshida, F. Elastic and plastic properties of GaN determined by nano-indentation of bulk crystal. *Appl. Phys. Lett.* **1999**, *75*, 2070. [CrossRef]
28. Kese, K.O.; Li, Z.C.; Bergman, B. Method to account for true contact area in soda-lime glass during nanoindentation with the Berkovich tip. *Mater. Sci. Eng. A* **2005**, *404*, 1–8. [CrossRef]
29. Kavouras, P.; Ratschinski, I.; Dimitrakopulos, G.P.; Leipner, H.S.; Komninou, P.; Leibiger, G.; Habel, F. Deformation and fracture in (0001) and (10-10) GaN single crystals. *Mater. Sci. Technol.* **2018**, *34*, 1531–1538. [CrossRef]
30. Huang, J.; Xu, K.; Fan, Y.M.; Wang, J.F.; Zhang, J.C.; Ren, G.Q. Dislocation luminescence in GaN single crystals under nanoindentation. *Nanoscale Res. Lett.* **2014**, *9*, 649. [CrossRef] [PubMed]
31. Jian, S.-R.; Juang, J.-Y. Nanoindentation-induced pop-in effects in GaN thin films. *IEEE Trans. Nanotechnol.* **2013**, *12*, 304. [CrossRef]
32. Bradby, J.; Williams, J.; Swain, M. Pop-in events induced by spherical indentation in compound semiconductors. *J. Mater. Res.* **2004**, *19*, 380. [CrossRef]
33. Jian, S.-R. Berkovich indentation-induced deformation behaviors of GaN thin films observed using cathodoluminescence and cross-sectional transmission electron microscopy. *Appl. Surf. Sci.* **2008**, *254*, 6749. [CrossRef]
34. Nix, W.D.; Gao, H. Indentation size effects in crystalline materials: A law for strain gradient plasticity. *J. Mech. Phys. Solids* **1998**, *46*, 411. [CrossRef]
35. Wang, R.; Fang, Q.F. Core structure and mobility of an edge dislocation in aluminum. *J. Alloys Compd.* **2000**, *310*, 80. [CrossRef]
36. Fang, Q.F.; Wang, R. Atomistic simulation of the atomic structure and diffusion within the core region of an edge dislocation in aluminum. *Phys. Rev. B* **2000**, *62*, 9317. [CrossRef]
37. Liu, W.; Chen, L.; Cheng, Y.; Yu, L.; Yi, X.; Gao, H.; Duan, H. Model of nanoindentation size effect incorporating the role of elastic deformation. *J. Mech. Phys. Solids* **2019**, *126*, 245. [CrossRef]
38. Huang, J.; Xu, K.; Gong, X.J.; Wang, J.F.; Fan, Y.M.; Liu, J.Q.; Zeng, X.H.; Ren, G.Q.; Zhou, T.F.; Yang, H. Dislocation cross-slip in GaN single crystals under nanoindentation. *Appl. Phys. Lett.* **2011**, *98*, 221906. [CrossRef]
39. Qiu, X.; Huang, Y.; Nix, W.D.; Hwang, K.C.; Gao, H. Effect of intrinsic lattice resistance in strain gradient plasticity. *Acta Mater.* **2001**, *49*, 3949. [CrossRef]
40. Qian, Y.; Shang, F.; Wan, Q.; Yan, Y. A molecular dynamics study on indentation response of single crystalline wurtzite GaN. *J. Appl. Phys.* **2018**, *124*, 115102. [CrossRef]
41. Han, S.M.; Feng, G.; Jung, J.Y.; Jung, H.J.; Groves, J.R.; Nix, W.D.; Cui, Y. Critical-temperature/Peierls-stress dependent size effects in body centered cubic nanopillars. *Appl. Phys. Lett.* **2013**, *102*, 041910. [CrossRef]
42. Wheeler, J.M.; Michler, J. Indenter materials for high temperature nanoindentation. *Rev. Sci. Instrum.* **2013**, *84*, 101301. [CrossRef] [PubMed]

43. Xiao, X.; Terentyev, D.; Ruiz, A.; Zinovev, A.; Bakaev, A.; Zhurkin, E.E. High temperature nano-indentation of tungsten: Mod-elling and experimental validation. *Mater. Sci. Eng. A* **2019**, *743*, 106. [CrossRef]
44. Tromas, C.; Audurier, V.; Leclerc, S.; Beaufort, M.F.; Declémy, A.; Barbot, J.F. Evolution of mechanical properties of SiC under helium implantation. *J. Nucl. Mater.* **2008**, *33*, 142. [CrossRef]

Disclaimer/Publisher's Note: The statements, opinions and data contained in all publications are solely those of the individual author(s) and contributor(s) and not of MDPI and/or the editor(s). MDPI and/or the editor(s) disclaim responsibility for any injury to people or property resulting from any ideas, methods, instructions or products referred to in the content.